

Design of an e-Health Respiration and Body Posture Monitoring System and its Application for Rib Cage and Abdomen Synchrony Analysis

Atena Roshan Fekr, Katarzyna Radecka and Zeljko Zilic

Department of Electrical and Computer Engineering, McGill University, Montreal, Canada
 atena.roshanfekr@mail.mcgill.ca, {katarzyna.radecka, zeljko.zilic}@mcgill.ca

Abstract— Automated methods of real-time and unobstructive patient's respiration and position monitoring have been subjects of interests in e-health applications. The present study implements a low-cost and convenient monitoring system for patients with breathing problems or sleep disorders. We have also captured the Rib Cage (RC) and Abdomen (AB) movements using accelerometer sensors. In addition to measurement of phase shift between the chest wall compartments, the impacts of different body positions on AB and RC motions have been investigated. The performance of the presented system is evaluated and the average Mean Square Error (MSE) of 0.14 is achieved for three breath timing variables. Moreover, the overall errors of phase angles for paradoxical and synchronous breath patterns are $0.25^\circ \pm 0.06$ and $0.26^\circ \pm 6E-03$, respectively. The system properly indicates a significant increase in the degree of ribcage and abdomen asynchrony in the paradoxical breathing compared to normal pattern.

Keywords—respiration; body posture; accelerometer; Bluetooth Low Energy; rib cage; abdomen

I. INTRODUCTION

Remote monitoring of respiratory parameters such as inspiratory time (T_i), expiratory time (T_e), and total time of the respiratory cycle (T_{tot}) as well as respiration rate (RR) [1] is an important diagnostic method in planning of medical care. All these parameters can be measured by direct methods which require breathing through some measuring apparatus such as spirometer, or need medical expertises for implementing the devices such as Optoelectronic plethysmography (OEP). Regardless of their accuracy, these techniques are uncomfortable and are not practical to be integrated in body sensor network for continuous monitoring from the outside hospital environments [2].

An indirect method of breath analysis is based on the blood concentration of oxygen. This technique does not provide a reliable indication of changes in breathing pattern while has slow reaction to breath disturbance as well [2]. Another indirect method is based on measurements of tracheal breath sounds. Although it is an efficient method for detecting deep and low breathing sound amplitude, it does not exceed the background noise whereas the relationship between the sound amplitude and air flow is very difficult to detect [3]. [4] provides a literature review on Optoelectronic plethysmography (OEP) as an indirect measurement of pulmonary ventilation. They applied 89 passive markers which were placed on important body points with a sampling frequency of 50Hz. Four CCD cameras are used to capture the

3D coordinates of each marker. The cameras operate at up to 120Hz and are synchronized with axial diodes that emit infrared light. The system showed good intra – and inter-rater reliability, with correlation coefficients above 0.75 for most of the analyzed variables. OEP also used for movement analysis of rib cage and abdomen. Even though, OEP is a new reliable method for breath analysis, it is impossible to use it for remote monitoring of respiratory parameters since the use of OEP requires laborious and complex calibration procedures. One recent area of interest is applying motion sensors to detect the small movements of the body that occur during expansion and contraction of the lungs. A validation of respiratory signal derived from suprasternal, notch acceleration has been investigated by [5] for three different body positions *i.e.* supine, left side and prone. They show that there is a high correlation between accelerometer driven respiration and spirometry in all conditions. Their data storage and processing are performed on a computer with a custom build LabVIEW Virtual Instrument. In [6] the respiratory component are achieved with the accelerometer mounted on the suprasternal notch of subjects in supine position. Their results represent the feasibility of implementing an accelerometry-based portable device for respiration recording. The data acquisition is done with a compact system and a laptop where data were stored to be used later.

The main objective of this study is to provide a new cloud-based platform for monitoring respiration patterns of the patients with accelerometer sensor. The previous systems often require a laptop, memory card or handheld PC to be carried by the subject due to the processing, data storage, and power requirements of the sensory equipment. However, in our system we use cloud database which can offer significant advantages over traditional methods, including increased on-line accessibility, scalability, automatic failover and fast automated recovery from failures. In addition to real time monitoring of different respiration parameters, the doctors are able to track the patient's body position and angle during sleep or at rest in different conditions. It is worth noting that, sleep position is a clinically applicable parameter that must be taken into account for several sleep disorders [7]. For instance, studies have shown the effectiveness of sleeping on your side, called "positional therapy", for mild to moderate positional Obstructive Sleep Apnea (OSA) [8][9]. Besides, [10] demonstrated that before and after parturition, the body movements and positions during sleep have statistically major differences. For people suffering from gastroesophageal reflux (GER) the left lateral position is preferable [11]. Therefore the

possibility of acquiring both respiration parameters and patients positions from one device gives more credits to accelerometer-based approaches as a simple and cost effective solution for remote monitoring applications.

The assessment of respiratory pattern can be done in different ways, from visual observation to three-dimensional (3D) analysis of Rib Cage (RC) and Abdomen (AB) movements [4]. Therefore, in the next part of this study we have analyzed the AB and RC motions by capturing the data of two accelerometer sensors in five different body positions. The data are used for synchronous and paradoxical breathing patterns classifications as well as demonstrating the effect of body positions on RC and AB synchronizations. Asynchronous movement of Rib cage-abdominal is often evident during loaded breathing and is known as a symptom of failure to wean from mechanical ventilation [12]. Moreover, the phase difference between RC and AB is utilized for Obstructive Sleep Apnea (OSA) diagnosis. Based on [13] the OSA was characterized by paradoxical motion of the RC or AB in 91% of patients. Thus the proposed remote monitoring platform can avoid invasive monitoring methods that can adversely affect sleep.

In our proposed platform, the accelerometer data is transmitted via Bluetooth Low Energy (BLE) to PC/Smartphone and then is sent to the cloud to be processed and saved, immediately. It is worth mentioning that in case of network disconnection, the data is saved on the intermediate interface such as tablets. Therefore, the physicians can track the patients wherever they are with devices such as an iPhone, iPad or the web regardless of their proximity to the patients. Moreover, we could obtain an accurate estimation of respiration waveform and parameters such as T_i , T_e and T_{tot} in different postures. Since, to the best of our knowledge, there is no accurate accelerometer based device to distinguish the synchronous and paradoxical breathing patterns, in this paper we aim to propose a platform in which two accelerometer sensors are applied. It not only extracts the respiration parameters and body positions, but also diagnoses the breath disorder from outside of medical centers. Fig. 1 briefly describes the overall view the proposed respiration monitoring platform.

In section II, a technique is presented to accurately measure the Pearson correlation of accelerometer driven respiration signal against the spirometer as well as calculation of respiration parameters. In section III, the body angles and positions have been investigated from the accelerometer signal. The synchronous and paradoxical breathing patterns are analyzed by the proposed remote platform in section IV. To the best of our knowledge, it is the first time that the synchrony of the rib cage compartments is investigated based on the acceleration movement of the body in a portable respiration platform. Experimental results are presented and discussed in Section V. Finally Section VI concludes the paper.

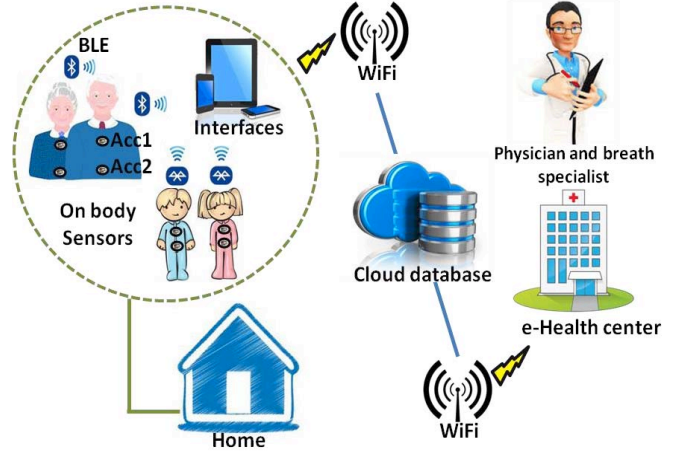


Fig. 1. Overall view of the proposed remote cloud-based respiration monitoring platform

II. ACCELEROMETER DRIVEN RESPIRATION SIGNAL AND PARAMETERS

In this section, a procedure is described to calculate the correlation of accelerometer driven signal with a reference spirometer in different body positions. In order to deliver high accuracies for the sensor measurements, we perform a calibration technique using least square method proposed by [14].

Calibration, which is defined as the process of mapping raw sensor readings into corrected values [15][16], is critical in medical applications due to inherent deficiency or aging problems. Generally, different special tools with specialists experiences are required for sensors calibration; however, a straightforward method to calibrate an accelerometer is performed at 6 stationary positions [14]. We need to collect a few seconds of accelerometer raw data at each position. Then the least square method is applied to obtain the 12 accelerometer calibration parameters. The calibration procedure is simple, and needs to be executed once. The calibration procedure can be briefly explained as follows:

$$[a_{x'}, a_{y'}, a_{z'}] = [a_x \ a_y \ a_z \ 1] \cdot \begin{bmatrix} acc_{11} & acc_{21} & acc_{31} \\ acc_{12} & acc_{22} & acc_{32} \\ acc_{13} & acc_{23} & acc_{33} \\ acc_{10} & acc_{20} & acc_{30} \end{bmatrix}$$

$$\mathbf{y} = \mathbf{w} \cdot \mathbf{X}$$

Where:

- Vector \mathbf{w} is accelerator sensor raw data collected at 6 stationary positions
- Vector \mathbf{y} is the known normalized Earth gravity vector.
- Matrix \mathbf{X} is the 12 calibration parameters that is determined as below:

$$\mathbf{X} = [\mathbf{w}^T \cdot \mathbf{w}]^{-1} \cdot \mathbf{w}^T \cdot \mathbf{y}$$

During a normal respiration, in each breathing cycle the volume of the thoracic cavity is changed, resulted from the displacements of the rib cage and diaphragm. Hence, we employ an accelerometer sensor mounted on the subject's chest (Acc1) to capture the movement of the rib cage while also providing more comfort compared to other locations, such as suprasternal notch. To analysis the rib cage and abdomen movements at the same time, our second sensor (Acc2) is attached on the subjects' umbilical region. Both sets of signals were captured synchronously at 50Hz, and were digitally low-pass filtered with a 1Hz cutoff frequency with which some high-frequency noises can be removed.

Fig. 2(a) depicts a part of respiration flow from spirometer for the normal breathing pattern of a 29 years old man in resting position. We apply a numeric integration algorithm in which the trapezoidal rule was used to estimate the area under the flow curve and obtain the respiratory volume drawn in black in Fig. 2(b), (c). The red line in Fig. 2(b) and (c) denotes the respiration signal from Acc1. Both accelerometer and spirometer are sampling with equal rate 50Hz. However, as can be seen in Fig. 2(b) there is cumulative time delay between the reference respiration signal and the output signal from our hardware module. In order to obtain the correlation of our proposed accelerometer driven respiratory signal with spirometer, first we need to remove this phase delay affected on their synchronization. We found out that this type of error on signals is due to different sampling frequencies which resulted from different architecture of the measurement units. Thus, to calculate the correlation, it is essential to ensure that

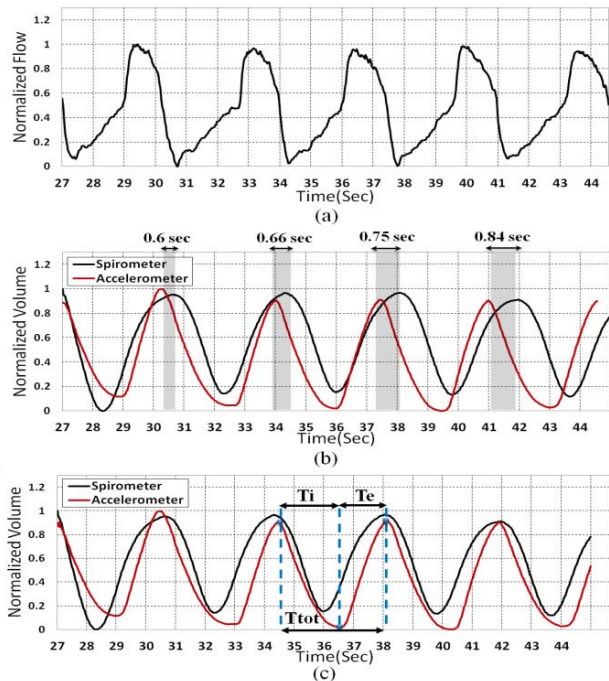


Fig. 2. (a) The normalized flow of spirometer, (b) The cumulative error of accelerometer and spirometer normalized volume signals over time before resampling (c) Two signals after resampling procedure.

both signals have identical frequencies. For this purpose after rational fraction estimation, we resample our data by an anti-aliasing low pass FIR filter during the resampling process.

In our experiments, the sampling rate of the accelerometer sensor was set to 50Hz, however; the data was logged with about 51Hz (measured frequency). With resampling process explained above, we could compensate the time lead about 0.02 per second (Fig.3). Note that the system automatically checks the number of samples in each analysis window to find the measured frequency of the sensor. Then the peak of their cross correlation is obtained for finding the best starting point between two respiration signals. Now, the correlation can be computed based on the following formula.

$$R_{A,S} = \frac{x(\sum_{i=1}^x A_i S_i) - (\sum_{i=1}^x A_i)(\sum_{i=1}^x S_i)}{\sqrt{[x \sum_{i=1}^x A_i^2 - (\sum_{i=1}^x A_i)^2][x \sum_{i=1}^x S_i^2 - (\sum_{i=1}^x S_i)^2]}}$$

Where A and S denotes the accelerometer sensor data and spirometer with x samples, correspondingly.

We have also calculated per breath inspiratory time (T_i), expiratory time (T_e), and total time of the respiratory cycle (T_{tot}) from the accelerometer driven respiration waveform by peak and valley detections, described in Fig. 2 (c). The applied peak/valley detector defined a customized threshold to decide whether each peak (or valley) is significantly larger (or smaller) than the local data.

III. BODY POSITION AND ANGLE CALCULATION

Body position is an important parameter that must be considered for several sleep disorder problems. For example, Fernandes *et.al* investigates the impact of the body position and obstructive sleep apnea in children. He concludes that, unlike adults, children with OSA breathe best when in the supine position [17]. Moreover, sleeping on the back has been suggested by the American Academy of Pediatrics in 1992 to avoid Sudden Infant Dead Syndrome. SIDS decreased dramatically in some countries where the "Back to Sleep" recommendation has been widely adopted, such as the U.S. and New Zealand [18].

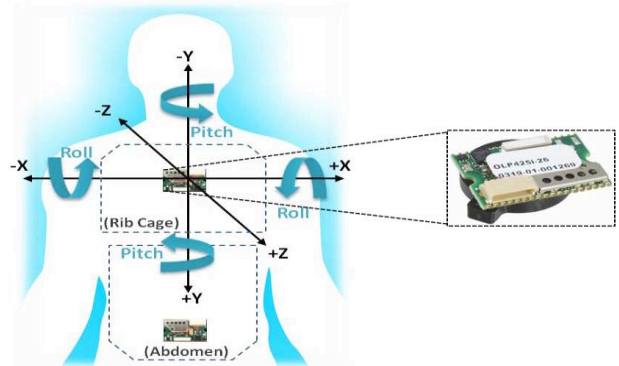


Fig. 3. The accelerometer sensors placements on the body and tilt angles

The method described in this paper helps to identify the rest and sleeping positions with the representation of roll and pitch angles. For a stationary object, the pitch and roll angles can be obtained with 3-axis accelerometer [19]. This method is also very useful in calibrating accelerometer sensor to improve the readouts accuracy as we discussed earlier. We measure the tilt angles with trigonometric formulas as follows [14] (see Fig. 3):

$$\text{Pitch} = \alpha = \arctan\left(\frac{a_{x_i'}}{\sqrt{a_{y_i'}^2 + a_{z_i'}^2}}\right)$$

$$\text{Roll} = \beta = \arctan\left(\frac{a_{y_i'}}{\sqrt{a_{x_i'}^2 + a_{z_i'}^2}}\right)$$

Where $a_{x_i'}$, $a_{y_i'}$ and $a_{z_i'}$ are calibrated data of 3-axis accelerometer. In this paper five different body positions are evaluated and the corresponding body angles are defined in Table I.

TABLE I. CONSIDERED PITCH AND ROLL ANGLES FOR FIVE DIFFERENT POSITIONS BASED ON THE SENSOR LOCATION

Postures/Angles	Pitch (Degree)	Roll (Degree)
Sitting	0 °	-90 °
Resting	0 °	-45 °
Supine	0 °	0 °
Left side	+90 °	0 °
Right side	-90 °	0 °

IV. BREATH SYNCHRONIZATION ANALYSIS

In this part, we analyze the synchronous and asynchronous breathing patterns with our accelerometer sensors. For this goal, the chest wall is modelled in two compartments: Rib Cage (RC) and abdomen (AB) shown in Fig. 3. Indeed in healthy people, the inspiration occurs by cause of systematic actions of the diaphragm and intercostal muscles which resulted in RC and AB expansion synchronously during spontaneous breathing at rest. Asynchronous breathing, in

contrast, is defined as the difference in time of expansion or retraction between the compartments of the chest wall [20][21]. However, in case of extreme phase differences, the movement among the compartments becomes opposite, and then the paradoxical movement occurs [22]. For example, according to the studies [23]-[25], paradoxical behaviour of the chest wall is recognized in patients with Chronic Obstructive Pulmonary Disease (COPD).

In this section the phase shift between AB and RC are calculated based on the degree of opening of Lissajous figure or Konno-Mead loop on accelerometer driven respiration signals [4]. The phase angle (θ) is measured in degrees ($^\circ$), changing from 0° to 180° . 0° and 180° represent the perfect synchronous pattern and paradoxical movement of the chest wall compartments, respectively. In Lissajous figure, the movements of one compartment are plotted versus the excursion of the second compartment in an X-Y graph during a single respiratory cycle [26][27]. θ is defined by the following formula:

$$\theta = \sin^{-1} \frac{m}{s}$$

Where s represents the V_T of the signal on the X-axis and m is the distance between the two intercepts of the loop with the ordinate at abscissa equal to 50% of the V_T of the signal on the Y-axis [28]. If the slope of the main diagonal of the loop is negative e.g. in paradox breathing (Fig. 4(c)), the phase angle is greater than 90° , thus:

$$\theta = 180 - \vartheta, \sin \vartheta = m/s$$

Here, after signal processing described earlier, the respiration signals derived from both sensors are normalized with respect to time. Then the phase angles are calculated from their Lissajous figures as depicted in Fig. 4. The figure shows the Lissajous figure of one of our subjects in resting position during his normal and paradoxical breathing. The

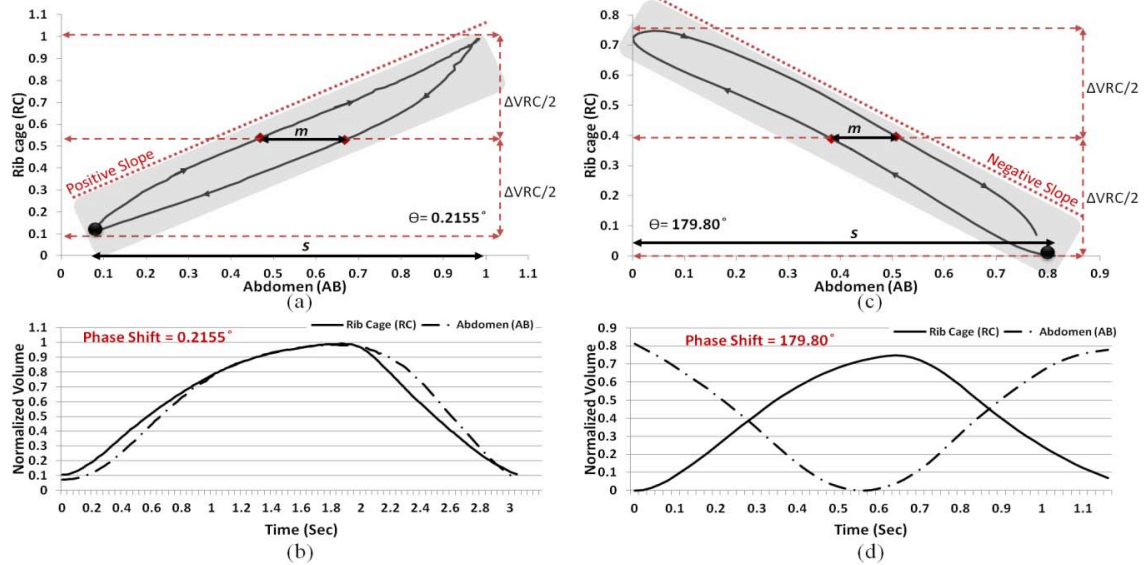


Fig. 4. (a) The Lissajous figure of normal breathing of one subject, (b) the normalized volume derived from the accelerometer sensors mounted on the chest and abdomen in normal pattern, (c) the Lissajous figure of paradoxical breathing and (d) the normalized volume derived from the accelerometer sensors mounted on the chest and abdomen in paradoxical pattern

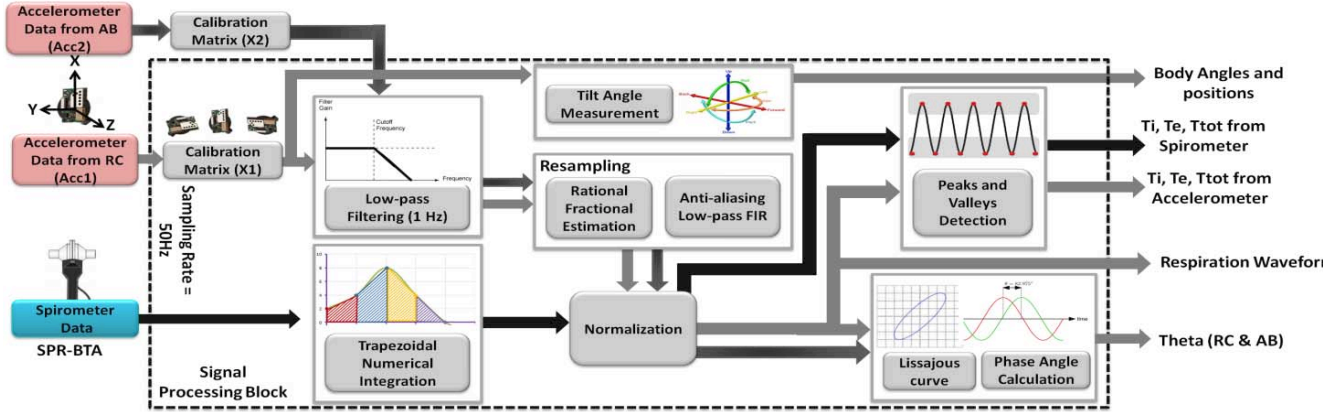


Fig.5. Proposed respiration monitoring procedures

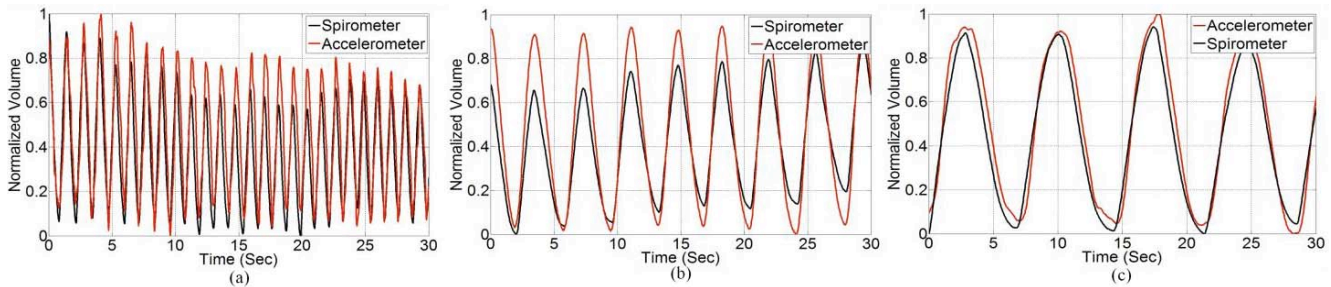


Fig.6. (a) Fast, (b) normal and (c) slow respiration patterns

solid dot corresponds to the onset of inspiration and arrows denote the direction of the loop. The phase shift between his RC and AB in this breath cycle for normal breathing is calculated as 0.2155° while in his paradoxical breathing shown in Fig. 4(c) and (d) it is calculated as 179.80° which indicates a significant increase in the degree of ribcage and abdomen asynchrony. Besides, we have investigated the impact of posture and body angle on the synchronization of RC and AB in both normal and true paradoxical breathing maneuvers. All procedures of the proposed respiration monitoring platform are summarized in Fig. 5. The experimental results are described in section V in more details.

V. EXPERIMENTAL RESULTS

A. Test setup

The participants of this study were 4 healthy females and 3 healthy males aged 19 to 46 with (Mean \pm SD) 28.85 ± 8.76 . They were instructed how to perform each breath exercise before their recording sessions. The experimental trials lasted for about 80 minutes per subject. We asked the subjects to perform normal, fast, slow and paradoxical patterns, each for 1 minute (3000 samples), in five different body positions: sitting, resting, supine, left side and right side. We assigned a 3-minute rest interval after performing each pattern. Based on the definitions, for normal breathing we consider 12 to 20 rpm, in slow pattern less than 12 rpm and for fast breathing the subjects are asked to breathe more than 20 respirations per minutes. For simulating paradoxical breathing we instructed the subjects to reverse their abdomen movement in inhalation and exhalation. There was no limitation in the number of

respiration for paradoxical breathing maneuver. In our system we used a 22.3×14.8 mm, cB-OLP425 Bluetooth low energy module, which is fully radio type approved for Europe, USA and Canada as well as compliant with EMC safety and medical standards [29]. This module includes an ultra low-power LIS3DH 3-axis accelerometer with 12-bit resolutions. The sensor was mounted on the subject's chest in the middle of sternum region and secured by a soft and elastic strap which is easy to attach and comfortable to wear. In paradoxical breath experiments our second sensor is attached on the subjects' umbilical region. In our tests, both sensors are sampling with 50HZ rate. The SPR-BTA spirometer signal is used as our reference which measures the oral breathing. A nose clip was used to prevent nasal breathing during recordings. The Go!Link USB sensor interface is used as the data logger of our spirometer.

B. Accelerometer driven respiration signal validation

In this section, first the correlation between the spirometer and accelerometer signal is calculated on 7 different subjects with various ages, each for three types of respiration listed in Fig. 6 conducted in 5 different body positions. The results are brought in Table II. It is worth noting that based on the body movement mechanism in different positions; the major axes could be chosen either Z or Y depending on the postures. The mean value of the correlation coefficient between accelerometer and spirometer for all subjects and conditions is 0.84 ± 0.1 which demonstrate a very close correspondence between two signals. Besides, per breath time variables through accelerometer and spirometer are: inspiratory time, expiratory time, and total time of the respiratory cycle. The

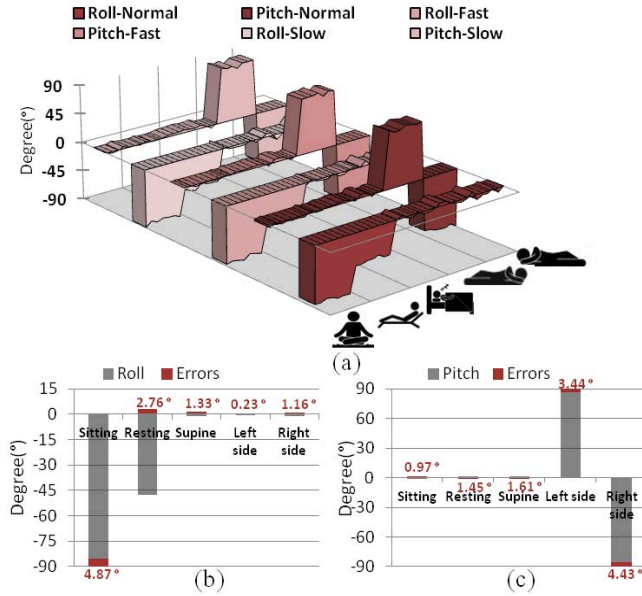


Fig.7. (a) Average Pitch and Roll angles on three respiration patterns for all subjects in different body positions, (b) average Roll angles of all subjects and patterns for five different positions with absolute errors in degree (c) average Pitch angles of all subjects and patterns for five different positions with absolute errors in degree

results of accelerometer driven respiration parameters are validated against the spirometer results and the average Mean Square Errors (MSE) for three breathing types are listed in Table III. The results also show the impact of body position on the correlation as well as time variables. For all subjects the mean correlation on different positions and breathing patterns are more than 0.8 shown in the last column of Table II. The average MSE obtained from all subjects and postures are 0.16, 0.17 and 0.09 for T_i , T_e and T_{tot} , correspondingly.

As described earlier, another potential application of the presented remote monitoring respiratory platform is the body position tracking. In our experiments, the subjects were asked to stay at specific angles described in Table I for different body positions. The average results of their body angles for slow, normal and fast patterns at the end of each experiment are shown in Table III. Since the subjects are kept in specific positions during the experiment, our system reports 2.07° average displacement in Pitch and 2.38° in Roll angles, which are negligible for body position detection at sleep or rest conditions. The average Pitch and Roll angles on normal, fast and slow breath patterns for all 7 subjects are presented in Fig. 7 (a). As an example, it could be observed that switching from sitting to rest position, angle α decreased in average from -85.12° to -47.76° (Fig. 7 (b)) while angle β almost kept 0 degree (changing from -0.97° to 1.45°). Similarly, angle β started to increase in positive range (in average from 1.61° to 86.56°) when patient changes his position from supine to left side shown in Fig. 7 (b).

C. Results of breath synchronization analysis

In this part of the paper, we have analyzed the accelerometer driven respiration signals from both rib cage

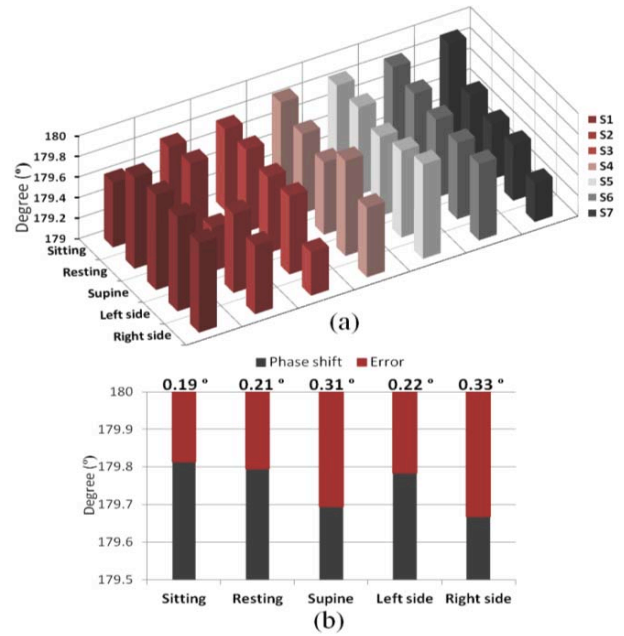


Fig.8. Average θ (a) for different body positions on three selected paradoxical breath cycles for all subjects (b) on all subjects for different body positions

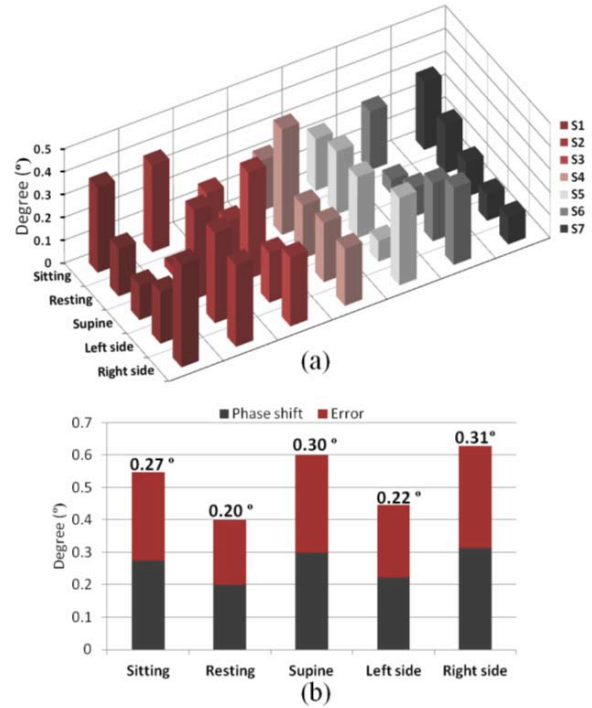


Fig.9. Average θ (a) for different body positions on three selected normal breath cycles for all subjects (b) on all subjects for different body positions

and abdomen, simultaneously. The impact of the body positions on RC and AB movements have been evaluated as well. Different studies show the importance of body posture on RC and AB movements. For instance, according to [30], in approximately one-half of the COPD patients, the RC and AB paradox was noticed while sitting; however this was not

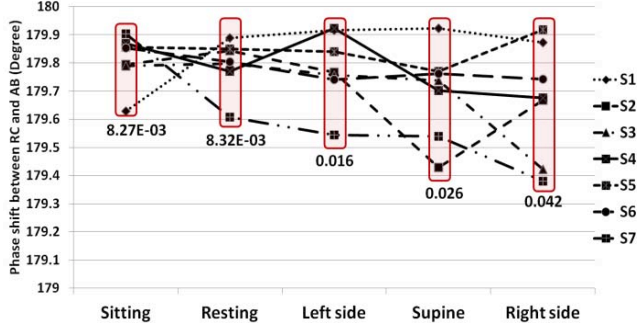


Fig.10. The phase angle between RC and AB compartments of different positions with the variances

related to impaired diaphragm motion. In contrast, in supine position, the rib cage paradox disappeared which resulted from the improvement of the diaphragm mechanism. Therefore, in this study we aim to calculate the phase shift between RC and AB with low-cost and portable sensors along with high accuracy and performance. Here, we choose three different breaths from each individual in paradoxical and normal breathing maneuvers. Note that, since we have $\theta = 0^\circ$ and $\theta = 180^\circ$ for synchronous and paradoxical breathings, we test these two models in our system. The average phase shift measured from the Lissajous figure for different postures are shown in Fig. 8 (a) and Fig. 9 (a). The overall error for paradoxical experiments in all conditions is $0.25^\circ \pm 0.06$ derived from Fig. 8 (b). Similarly, for normal breathing in

which we expect to have $\theta = 0^\circ$, the average measured error in all body postures and subjects is obtained $0.26^\circ \pm 6E-03$ shown in Fig. 9 (b). The results show that, both sensors are feasible and provide reliable phase shift from the rib cage and abdomen acceleration motion measurements.

Fig. 10 demonstrates the phase angle between RC and AB compartments of different positions for 7 subjects. In this assessment, the effect of posture on the variability of the phase angle is obtained based on their variances depicted in Fig. 10. It is observed that, in case of performing paradoxical test, the greatest variability is belong to the right side position while in sitting position all subjects have very close phase angles resulted in the least variability value.

VI. CONCLUSION

In this paper, we discussed about different challenges in designing of a real-time remote respiration monitoring platform. Indeed, the proposed system is an integration of different critical respiratory parameters monitoring with prominent benefits of cost, convenience, patient comfort and quality of service. We show that there is a very close correspondence of the accelerometer driven respiration waveform and spirometer data in terms of both correlation and timing variables. Furthermore, the platform is capable of tracking the body position and tilt angles during rest positions and sleep. Since changing body position induces significant differences in the chest wall behavior, the impacts of different

TABLE II. CORRELATION VALUES OF SPIROMETER AND ACCELEROMETER FOR ALL SUBJECTS AND BODY POSITIONS

Subject ID	Age/ Gender	Body Positions															Average
		Sitting			Resting			Supine			Left side			Right side			
		Fast	Normal	Slow	Fast	Normal	Slow	Fast	Normal	Slow	Fast	Normal	Slow	Fast	Normal	Slow	
S1	46/F	0.97	0.85	0.91	0.79	0.71	0.74	0.91	0.80	0.83	0.78	0.80	0.72	0.79	0.72	0.97	0.82
S2	30/F	0.87	0.90	0.90	0.83	0.95	0.90	0.85	0.98	0.97	0.74	0.73	0.89	0.91	0.98	0.98	0.90
S3	29/F	0.83	0.96	0.63	0.90	0.98	0.92	0.97	0.97	0.97	0.68	0.56	0.81	0.83	0.89	0.96	0.86
S4	29/M	0.93	0.80	0.72	0.91	0.86	0.79	0.95	0.90	0.94	0.82	0.59	0.86	0.67	0.55	0.68	0.80
S5	28/M	0.86	0.95	0.93	0.63	0.86	0.63	0.75	0.92	0.77	0.91	0.84	0.87	0.90	0.88	0.72	0.83
S6	22/F	0.94	0.91	0.96	0.88	0.87	0.94	0.86	0.95	0.95	0.78	0.80	0.82	0.70	0.78	0.96	0.87
S7	18/M	0.78	0.79	0.94	0.73	0.82	0.84	0.76	0.75	0.98	0.74	0.76	0.71	0.76	0.82	0.88	0.80

TABLE III. AVERAGE MSE OF INSPIRATORY TIME (T_i), EXPIRATORY TIME (T_e), AND TOTAL TIME OF THE RESPIRATORY CYCLE (T_{tot}) ON THREE BREATH PATTERNS DERIVED FROM ACCELEROMETER VS SPIROMETER AND THE PITCH AND ROLL ANGLES DURING DIFFERENT BODY POSITIONS

Subject ID	Body Positions																		Average MSE T_i	Average MSE T_e	Average MSE T_{tot}		
	Sitting				Resting				Supine				Left side				Right side						
	MSE T_i	MSE T_e	MSE T_{tot}	Pitch Roll	MSE T_i	MSE T_e	MSE T_{tot}	Pitch Roll	MSE T_i	MSE T_e	MSE T_{tot}	Pitch Roll	MSE T_i	MSE T_e	MSE T_{tot}	Pitch Roll	MSE T_i	MSE T_e				MSE T_{tot}	Pitch Roll
S1	0.38	0.49	0.49	-1.00° -86.94°	0.42	0.55	0.03	1.69° -47.26°	0.08	0.08	0.06	2.53° -0.36°	0.01	0.01	0.01	87.21° -2.10°	0.01	0.01	5.4E-03	-81.51° 6.99°	0.18	0.23	0.18
S2	0.19	0.20	0.09	-0.12° -83.87°	0.21	0.11	0.08	-0.87° -49.60°	0.08	0.07	0.03	-0.62° 1.23°	0.17	0.18	0.07	85.02° 3.54°	0.03	0.07	0.04	-84.82° -4.39°	0.14	0.13	0.07
S3	0.58	0.42	0.04	-2.12° -84.77°	0.11	0.08	0.08	0.33° -49.83°	0.02	0.01	0.02	4.07° -2.09°	0.50	0.67	0.21	85.89° 3.44°	0.07	0.10	0.06	-86.56° -2.48°	0.26	0.26	0.08
S4	0.29	0.30	0.12	0.18° -84.74°	0.07	0.08	0.01	1.27° -45.24°	8.96E-03	0.01	8.73E-03	4.66° -3.22°	0.15	0.13	0.15	86.68° -3.25°	0.23	0.19	0.06	-85.37° -1.52°	0.15	0.14	0.08
S5	0.03	0.05	0.06	-0.77° -84.19°	0.06	0.04	0.02	1.84° -45.36°	0.10	0.11	0.04	0.47° -1.36°	-0.13	0.13	0.14	85.97° 1.12°	0.08	0.12	0.13	-85.09° -1.23°	0.08	0.09	0.08
S6	0.04	0.03	0.04	-1.02° -84.46°	0.01	0.01	0.01	2.57° -48.56°	0.18	0.16	0.01	-1.56° 0.10°	0.32	0.27	0.29	87.33° -2.29°	0.11	0.13	0.02	-84.32° -4.94°	0.13	0.12	0.07
S7	0.23	0.06	0.15	-1.92° -86.89°	0.01	0.02	8.56E-03	3.36° -48.49°	0.11	0.13	0.03	1.76° -3.58°	0.68	0.91	0.05	87.83° -2.09°	0.07	0.08	9.63E-03	-88.34° -0.57°	0.22	0.24	0.05
Average	0.25	0.22	0.14	-0.97° -85.12°	0.13	0.13	0.03	1.45° -47.76°	0.08	0.08	0.03	1.62° -1.32°	0.28	0.33	0.13	86.56° -0.23°	0.09	0.1	0.09	-85.57° -1.16°	0.16	0.17	0.09

postures (sitting, resting, supine, left side and right side) on rib cage and abdominal asynchrony in 7 subjects have been systematically investigated for the first time by two accelerometer sensors. As a potential future work, we can make use of sensor fusion and fault-detection methods to improve the accuracy and tolerance to faults in multi-sensor applications dealing with high risks and major uncertainties [31].

REFERENCES

- [1] A. Roshan Fekr, M. Janidarmian, K. Radecka, Z. Zilic, "A medical cloud-based platform for respiration rate measurement and hierarchical classification of breath disorders," *Sensors* 2014, 14, 11204-11224.
- [2] A. Bates, M.J. Ling, J. Mann, D.K. Arvind, "Respiratory rate and flow waveform estimation from tri-axial accelerometer data," *Body Sensor Networks (BSN)*, 2010 International Conference, 2010;
- [3] C.-L. Que, C. Kolmaga, L.-G. Durand, S. M. Kelly, and P. T. Macklem, "Phonopneumetry for noninvasive measurement of ventilation: methodology and preliminary results." *J Appl Physiol*, vol. 93, no. 4, pp. 1515-1526, Oct 2002.
- [4] V. Parreira, D. Vieira, M. Myrrha, I. Pessoa, S. Lage, R. Britto, "Optoelectronic plethysmography: a review of the literature", *Braz. J. Phys. Ther*, vol 16, n. 6, pp 439-453, Dec 2012.
- [5] P.K. Dehkordi, M. Marzencki, K. Tavakolian, M. Kaminska, B. Kaminska, "Validation of respiratory signal derived from suprasternal notch acceleration for sleep apnea detection," *Engineering in Medicine and Biology Society, EMBC*, International Conference of the IEEE, pp.3824-3827, 2011.
- [6] Morillo, D.S.; Ojeda, J.L.R.; Foix, L.F.C.; Jimenez, A.L. An Accelerometer-Based Device for Sleep Apnea Screening. *IEEE Trans. Inf. Technol. Biomed.* 2010, 14, 491-499.
- [7] Y. Xu, S. Guangmin, L. Wen-Yen, C. Wen-Cheng, "The design of a real-time accelerometer-based sleeping position monitoring system and its application on obstructive sleep apnea syndrome," *Systems and Informatics (ICSAI)*, pp. 1061-1066, May 2012.
- [8] R. Cartwright, "A comparative study of treatment for positional sleep apnea," *Sleep* vol 14, pp 456-552, 1991.
- [9] R. Jokic, "Positional therapy versus continuous positive airway pressure in patients with positional obstructive sleep apnea," *Chest*, pp 771-781, 1999.
- [10] L. Zhaoqin, J. Linlin, C. Wenxi, K. Keichiro, N. Tetsu, "Characterization of maternal body movement during sleep before and after parturition," *IEEE International Conference on Engineering in Medicine and Biology Society (EMBC)*, pp. 1503-1506, 2011.
- [11] R. M. Khoury, L. Camacho-Lobato, P. O. Katz, M. A. Mohiuddin, and D. O. Castell, "Influence of spontaneous sleep positions on nighttime recumbent reflux in patients with gastroesophageal reflux disease," *Am J Gastroenterol*, vol. 94, pp. 69-73, 1999.
- [12] J. Marini, C. Roussos, M. Tobin, N. MacIntyre, M. Belman, J. Moxham, "Weaning from mechanical ventilation," *Am Rev Respir Dis*, pp. 1043-1046, 1988.
- [13] B. Staats, H. Bonekat, Harris CD, K. Offord, "Chest wall motion in sleep apnea," *Am Rev Respir Dis*, pp 59-63, 1984.
- [14] STMicroelectronics group of companies, "Tilt measurement using a low-g 3-axis accelerometer", Application note, Canada, 2010.
- [15] A. Roshan Fekr, M. Janidarmian, K. Radecka, Z. Zilic, "Multi-Sensor Blind Recalibration in mHealth Applications", *IEEE International Humanitarian Technology Conference (IHTC)*, June 1-4, 2014, Montreal, Canada
- [16] A. Roshan Fekr, M. Janidarmian, O. Sarbishei, B. Nahill, K. Radecka, Z. Zilic, "MSE minimization and fault-tolerant data fusion for multi-sensor systems," In the *IEEE 30th International Conference on Computer Design*, pp. 445-452, Canada, 2012.
- [17] L. Fernandes do Prado, X. Li, R. Thompson, C. Marcus, "Body position and obstructive sleep apnea in children," *Sleep*, pp 66-71 2002.
- [18] E. Mitchell, L. Hutchison, A. Stewart, "The continuing decline in SIDS mortality," *Arch Dis Child*, pp 625-6, 2007.
- [19] M. Janidarmian, A. Roshan Fekr, K. Radecka, Z. Zilic, "Affordable eRehabilitation Monitoring Platform", *IEEE International Humanitarian Technology Conference (IHTC)*, June 2014.
- [20] M. Sackner, H. Gonzalez, M. Rodriguez, A. Belsito, D. Sackner, S. Grenvik, "Assessment of asynchronous and paradoxical motion between rib cage and abdomen in normal subjects and in patients with chronic obstructive pulmonary disease," *Am Rev Respir Dis.*, pp.88-93, 1984.
- [21] M. Tobin, T. Chadha, G. Jenouri, S. Birch, H. Gazeroglu, M. Sackner, "Breathing patterns. I. Normal subjects," *Chest*, 1983.
- [22] A. Aliverti, M. Quaranta, B. Chakrabarti, "Paradoxical movement of the lower ribcage at rest and during exercise in COPD patients," *Eur Respir J*, pp49-60, 2009.
- [23] E. Campbell, "Physical sign of diffuse airways obstruction and lung distension," *Thorax* vol 14, pp 1-3, 1969.
- [24] C. Hoover, "The diagnostic significance of inspiration movement of the costal margins," *Am J Med Sci*, pp 633-646, 1920.
- [25] J. Sharp, N. Goldberg, W. Druz, H. Fishman, J. Danon, "Thoracoabdominal motion in chronic obstructive pulmonary disease," *Am Rev Respir Dis*, pp 47-56, 1977.
- [26] J. Allen, M. Wolfson, K. McDowell, T. Shaffer, "Thoracoabdominal asynchrony in infants with airflow obstruction," *Am Rev Respir Dis*, 1990.
- [27] N. Kiciman, B. Andreasson, G. Bernstein, F. Mannino, W. Rich, C. Henderson, "Thoracoabdominal motion in newborns during ventilation delivered by endotracheal tube or nasal prongs," *Pediatr Pulmonol*. 1998.
- [28] E. Agostoni, P. Mognoni, "Deformation of the chest wall during breathing efforts," *J Appl Physiol*, 1966.
- [29] <http://www.connectblue.com>
- [30] R. Priori, A. Aliverti, A. Albuquerque, M. Quaranta, P. Albert, "The effect of posture on asynchronous chest wall movement in COPD," *J Appl Physiol*, 2013.
- [31] O. Sarbishei, M. Janidarmian, A. Roshan Fekr, B. Nahill, K. Radecka, Z. Zilic, "Multi-sensory System Integration Dependability", Chapter 18 in *Book Technologies for Smart Sensors and Sensor Fusion*, edited by K. Yallup and K. Iniewski, pp. 319-335, 2013.